5-2022

Characteristics of Mesospheric Temperature and Gravity Waves over Chile in 2020-2021

Damien M. Devitt
Utah State University

Kenneth Zia
Utah State University

Characteristics of Mesospheric Temperature and Gravity Waves over Chile in 2020-2021

By Damien M. Devitt, Yucheng Zhao, Mike Taylor, Kenneth Zia, Dominique Pautet

Background:

Gravity waves (GWs) are often confused with gravitational waves in the fabric of space time. However, there is a clear distinction between them. Gravity wave is a term used by the atmospheric research field to describe perturbations in the atmosphere. Gravity pulls the perturbations down and causes oscillations, these present in the form of waves. The best visualization is to think of ripples on a pond, as the ripple reaches its peak gravity pulls the ripple down and creates an oscillating effect.

Typically, GWs are caused by mountains where wind rushing over the mountain range creates perturbations above it. Other causes of GWs include large storms, where the low-pressure storm acts like the mountain and wind rushing overtop of the storm creates perturbations. There are many origins for GWs, but these are the most studied and well understood.

GWs in the atmosphere can break, depositing momentum and energy into the surrounding atmosphere. This changes the thermal and kinetic energy of surrounding molecules and therefore, the temperature and wind of the atmosphere. The purpose of this research is to understand characteristics of mesospheric temperature and gravity waves over Chile in 2020-2021. The mesosphere is an upper region of the atmosphere that ranges from 50 to 90 kilometers above sea level (Figure 1).

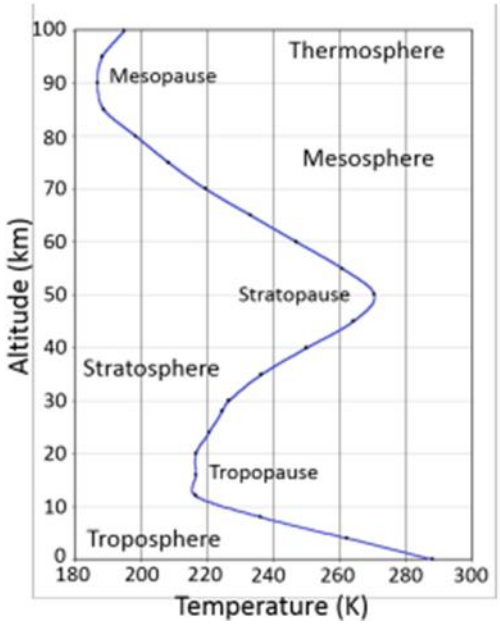

Fig 1. Vertical profile of atmospheric temperature in Kelvin, (borrowed from Pugmire's thesis).[1]

Instrumentation

The Utah State University (USU) Mesospheric Temperature Mapper (MTM) camera (Figure 3, right) takes images of the OH emission layer, located at a nominal height of 85 Km.[1] The camera has been in service since 2009 at the Andes Lidar Observatory (ALO), Located at Cerro Pachón, Chile (30.3°S, 70.7°W, 2530 m, Figure 2). The MTM camera was placed in the Andes Mountain range to capture GWs generated by wind blowing over the mountains.

Fig 2. Images of the Andes Lidar observatory (ALO) in Cerro Pachon, Chile (left) and the google map showing the location of ALO.

ALO MTM Temperature:

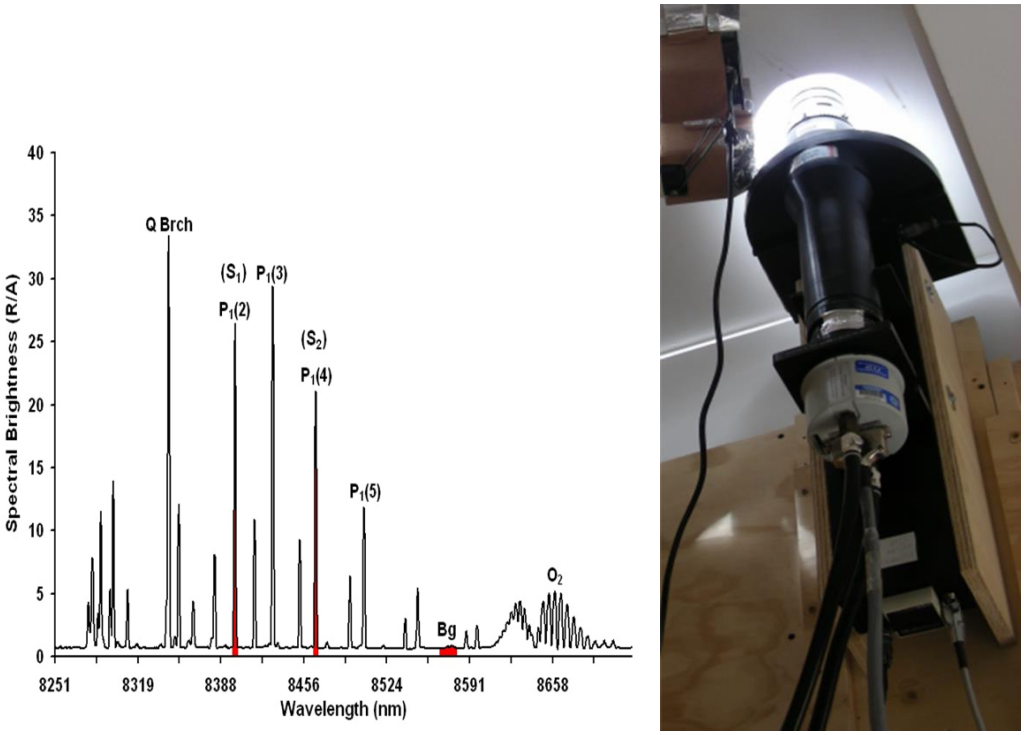

Fig 3. The band structure of NIR OH, highlighting the P1(2), P1(4), and BG bands used by the MTM camera (left) and a photo of the MTM camera at ALO (right).

The MTM camera takes images of the Near Infrared Hydroxyl (NIR OH) bands of the OH layer centered at ~87 Km, which is the upper region of the mesosphere and is the coldest part of the atmosphere (Figure 1). This region is one that has not been well studied as it is hard to get direction measurements of this region from above (satellite) and below (ground based). The MTM was specifically designed by USU to detect the OH airglow emission, more specifically the P1(2) and P1(4) emission lines in the OH (6,2) bands using ultra narrow bandwidth filters (Figure 2, left).[2] Through the ratio of the intensity of these two emission lines, temperature of the OH layer can be calculated.[3]

Instrument Specifications (Figure 2, right):

The specifications of the USU MTM are:

- Field of view ~90 degrees, (180 x 180 km)

- MTM is operated with sequential observations (30 sec. exp.) of:
    - Two emission lines (P1(2), P1(4)) in the NIR OH (6.2) Band and background (~857.5 nm)
- Cycle time: ~ 2 min per OH temperature determination. (Precision of ~2K)

MTM from ALO:

It should be noted that an electronic interference pattern is visible in the images, the most likely cause is the installation of an upgraded (more powerful) meteor radar that another research group uses at ALO (Figure 4). With the COVID-19 pandemic and current civil unrest going on in Chile, visiting the station has been impractical; a full diagnostic and repairs have not been possible. Due to the degrading insulation around the camera systems, the radar signal is now penetrating the MTM system causing the interference pattern in the OH images as shown in Figure 4.

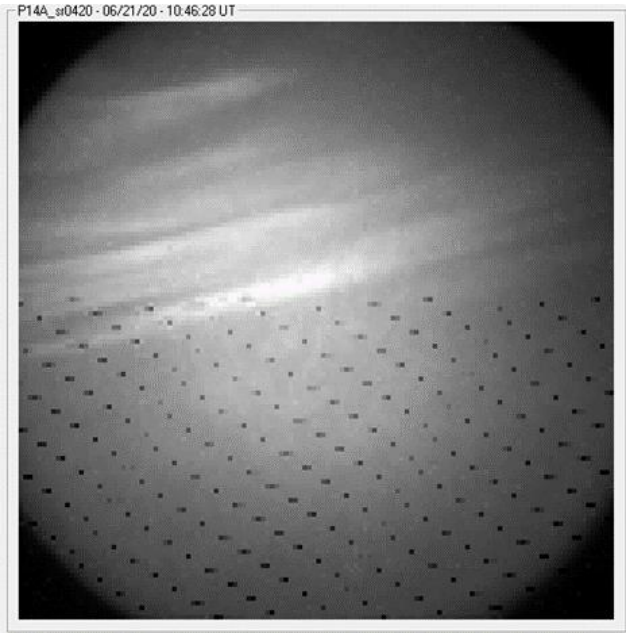

Fig 4. Sample raw image with noise caused by meteor radar (electronic) interference.

Analyzing the data found that electronic interference has drastically affected the imaging quality as 78.22% of 381 nights observed are plagued throughout most of the night with this electronic interference, leaving only 67 nights of clean data (Figure 5).

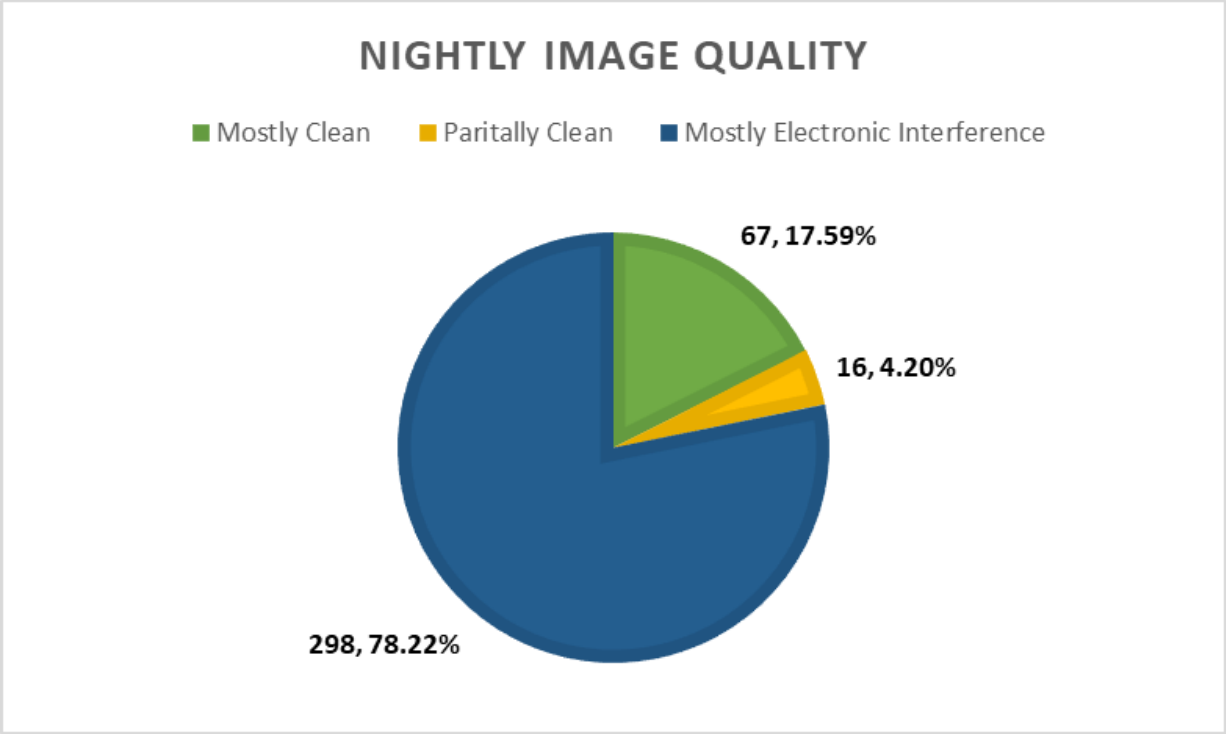

Fig 5. A pie chart showing the percentage of nights with completely clean, partially clean, or mostly electronic interference images throughout the entire night as a percentage of the total nights observed. Along with the number of nights in each category (shown to the left of each percentage. 17.59% mostly clean, 4.20% partially clean and 78.22% with interference.

MTM Data Analysis:

The process of analyzing the data involves, star removal, flat fielding, calibrating, unwarping ALO data (OH images) and generating the temperature and relative band intensity maps. These processes are necessary to be able to create a readable image from which valuable data like GW characteristics, such as phase speed, horizontal wavelength, direction of wave propagation, and zenith temperature can be obtained. The data allows further study of GW characteristics, and the possible origin of the waves in the troposphere.[4]

Star removal begins in the USU image processing program with the raw image shown in Figure 6 (left). The process calculates the intensity of each pixel within an image and the brightest pixels (stars) are replaced by the interpolated intensity value of nearby pixels (Figure

6, center). Flat fielding then removes variations from the background and distortions from the camera lenses by subtracting a calculated mean of images over the night.[1]

Calibrating uses known star maps to rotate the image so that true North is at the top of the image. This makes determining the propagation direction more apparent. Unwarping takes the warped image created by the cameras fisheye lens and flattens it into a 2D image of about 150 square kilometers (Figure 6, right).

After completing these analyses, two new maps are created. The rotational temperature map and band intensity map. These provide information about the gravity wave field in the part of the Mesosphere that's being observed.

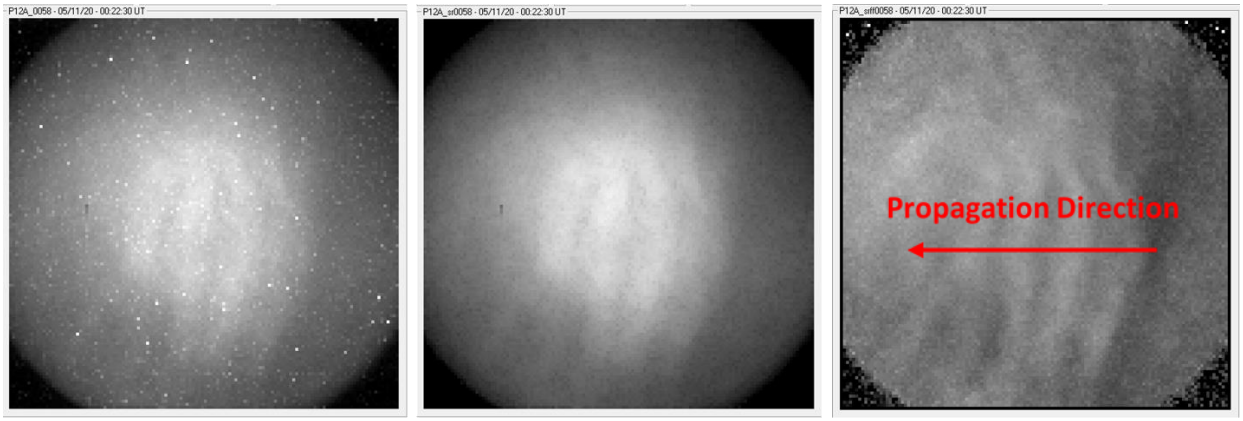

Fig 6. Left to right P1(2) images on May 10-11, 2020; raw, star removed, calibrated, and unwarped image containing a gravity wave.

Zenith temperature is calculated using the intensity Zenith or center 5x5 super pixels of the image. This results in a "straight-up" time series temperature for each image in a night. A nightly plot (Figure 7) is then produced and cleaned of outlier data due to the rising and setting of the sun using the "Origin" computer program.

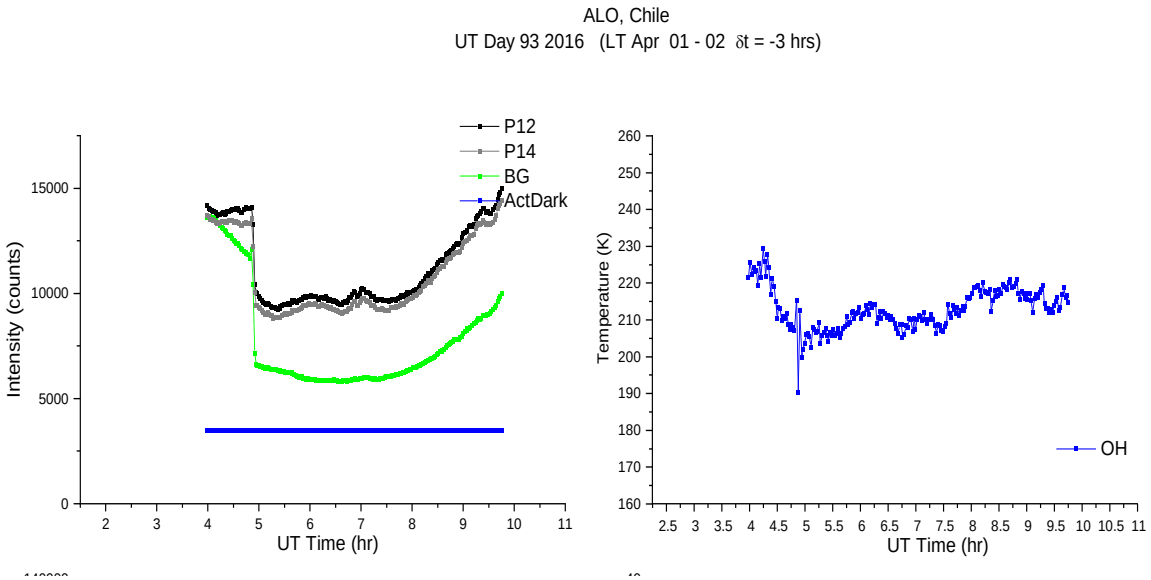

Fig 7. Uncleaned Zenith temperature graphs on the night of April 02-03, 2020, showing intensity in total counts (left). The emission lines P1(2) and P1(4) show wave activity, where the green line is the background intensity. The right graph shows a derived temperature for the night.[1]

Following this cleaning, a Python program engineered by myself and Kenneth Zia calculates the daily average temperature and translates it to a text file for the entire year. The "Origin" program is used again to generate a scatter plot with a 30-day running mean that was used to study the intra-seasonal mesospheric temperature variation over the Andes during 2020 (Figure 9).

GW events are characterized by date, time, wavelength, direction, and phase speed. Date and time portions are tied to the files themselves which are stamped. GW horizontal wavelength and propagating direction are calculated by the USU Image Processing program where an FFT is performed on the cleaned P1(2) files, an area of interest (AOI) is then chosen and the program performs the calculations (Figure 8, left).

The phase speed is calculated by using the distance a wave crest has moved over the course of chosen images. The red lines indicate the same wave crest over multiple images and the blue lines are the limits over which the calculation is performed (Figure 8, right). This provides the phase speed in m/s.

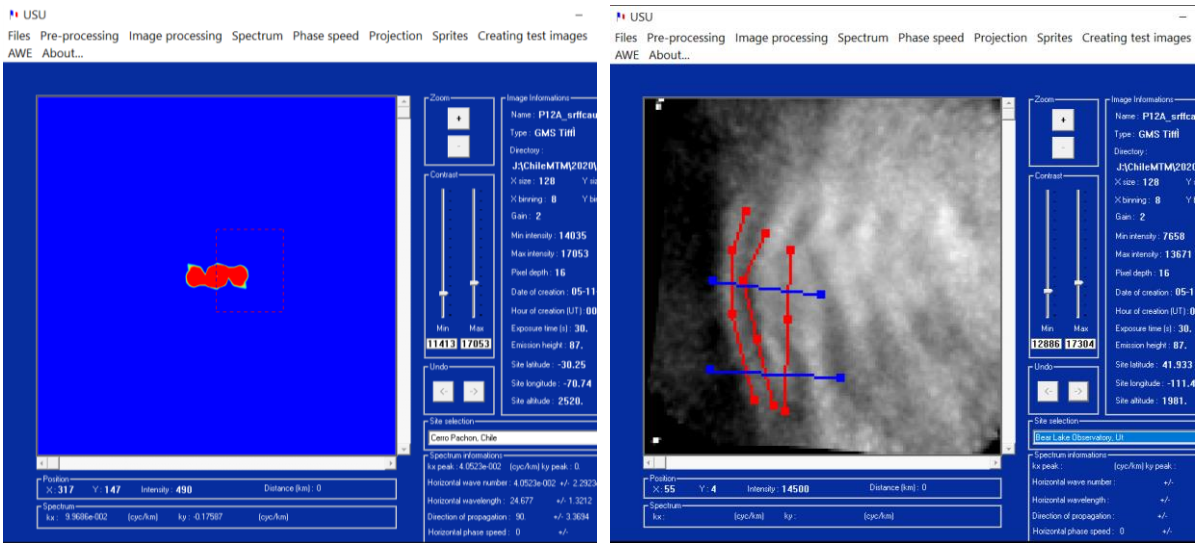

Fig 8. images showing the FFT for wavelength and propagation direction (left) and phase speed analysis technique (right) inside the USU Image Processing program on P1(2) files for May 10-11, 2020.

Results:

Mesospheric temperature variation

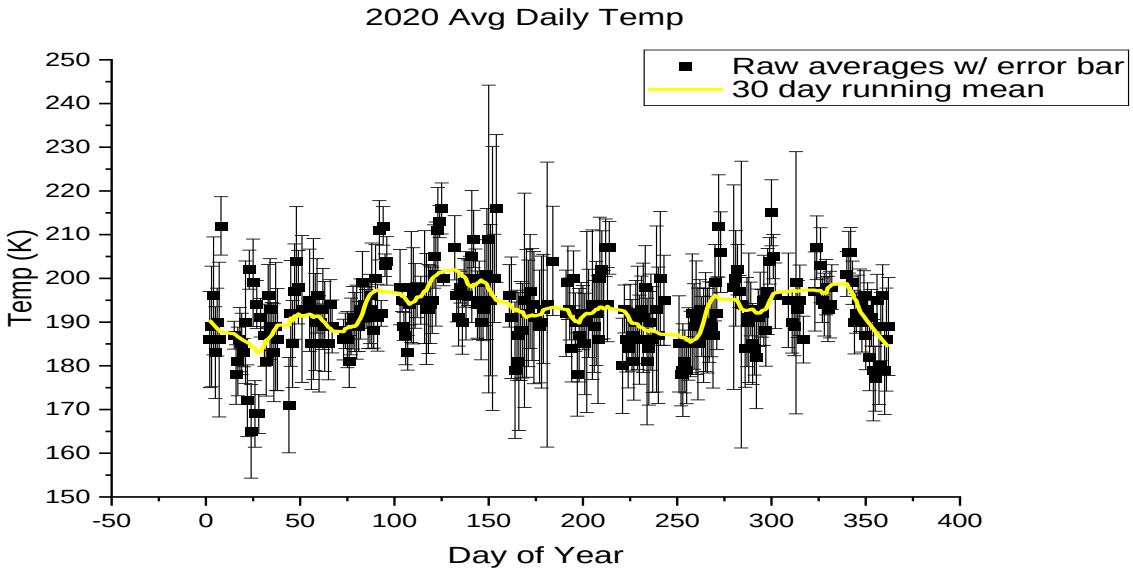

Fig 9. Scatter plot showing the average daily temperature for 2020 in black along with error bars, in yellow is a 30-day running mean that smooths the graph.

Figure 9 shows the nightly mean OH temperature of 2020, the yellow line indicates a 30-day running mean that shows seasonal characteristics. This data matches up well with previous

years, sharing similar features (Pugmire, 2018). Seasonal temperature variation was higher during the southern hemispheres winter months and lower during its summer months. The annual mean temperature was ~192 K with a variability of ~20 K in the mean. The black data points indicate the actual temperatures (squares) and the variability (error bars) are much larger.

Characteristics of mesospheric GWs during 2020 over ALO:

Finally, 7 nights containing GWs that were clean of interference and clouds were able to be analyzed. Using the USU Image Processing program the date, time, wavelength, direction, and phase speed were calculated for each wave event (Table 1). The GW events analyzed produced wavelengths of ~20-50 Km, phase speeds of ~15-160 m/s and durations of several minutes to nearly an hour. The characteristics of the GW event on May 10-11, 2020 are shown in Figures 6, 8 and are highlighted in red throughout this report.

Date (2020)	Time (UT)	Wavelength (Km)	Direction (degrees from north)	Phase speed (m/s)
Mar25-26	0:45-1:37	28	3.9	61.9
Apr02-03	3:59-4:47	20.4	7.6	24.5
Apr22-23	0:56-4:13	36.2	356.6	13.7
Apr29-30	2:37-4:53	30.7	26.6	14.6
May10-11	**23:18-1:37**	**25.7**	**270**	**19.1**
May22-23	3:44-4:45	22	0	26.5
May25-26	22:38-3:01	47.3	274.4	15.1

Table 1. Showing calculated characteristics of GWs for 7 distinct nights.

Conclusion:

MTM data from ALO between Jan. 1st, 2020 and May 31st, 2021 (~17 months) were analyzed and 7 GW events during 2020 were studied in this research. More GWs were observed during the nights when radar interference was present but for the reasons stated above, they were not analyzed. Following May 25-26, 2020, clean nights with waves became much rarer. The zenith temperature for 2020 shows an annual mean temperature of ~192 K with a similar seasonal variation as data from previous years. The GW events analyzed produced wavelengths

of ~20-50 Km, phase speeds of ~15-60 m/s and durations of several minutes to nearly an hour. The obtained data and results will be integrated into the long-term study being conducted at the ALO. New and better methods are currently being explored to speed up the analysis process and provide better data sets.

Acknowledgements:

This study is supported by NSF funding #1911970: “Collaborative Research: CEDAR--Airglow Imaging of Gravity Wave and Instability Dynamics”.

Bibliography:

[1] Pugmire, J. R. "Mesospheric Gravity Wave Climatology and Variances Over the Andes Mountains" (2018). All Graduate Theses and Dissertations. 7387.

[2] Pendleton, W.R. “Terdiurnal oscillations in OH Meinel rotational temperatures for fall conditions at northern mid-latitude sites” Geophysical Research Letters. Vol 27, NO. 12, pp. 1799 to 1802. June 15, 2000.

[3] Meriwether, J. W. “High latitude airglow observations of correlated short-term fluctuations in the hydroxyl Meinel 8-3 band intensity and rotational temperature” Planet. Space Sci. Vol. 23, pp. 1211 to 1221. Perpamon Press, 1975.

[4] Taylor, M. J. “Evidence of Preferential Directions for Gravity Wave Propagation Due to Wind Filtering in the Middle Atmosphere” Journal of Geophysical Research. Vol. 98, April 1, 1993.